Sprouty2 expression controls endothelial monolayer integrity and quiescence

Peier, Martin ; Walpen, Thomas ; Christofori, Gerhard ; Battegay, Edouard ; Humar, Rok

Abstract: Vascular integrity is fundamental to the formation of mature blood vessels and depends on a functional, quiescent endothelial monolayer. However, how endothelial cells enter and maintain quiescence in the presence of angiogenic factors is still poorly understood. Here we identify the fibroblast growth factor (FGF) antagonist Sprouty2 (Spry2) as a key player in mediating endothelial quiescence and barrier integrity in mouse aortic endothelial cells (MAECs): Spry2 knockout MAECs show spindle-like shapes and are incapable of forming a functional, impermeable endothelial monolayer in the presence of FGF2. Whereas dense wild type cells exhibit contact inhibition and stop to proliferate, Spry2 knockout MAECs remain responsive to FGF2 and continue to proliferate even at high cell densities. Importantly, the anti-proliferative effect of Spry2 is absent in sparsely plated cells. This cell density-dependent Spry2 function correlates with highly increased Spry2 expression in confluent wild type MAECs. Spry2 protein expression is barely detectable in single cells but steadily increases in cells growing to high cell densities, with hypoxia being one contributing factor. At confluence, Spry2 expression correlates with intact cell-cell contacts, whereas disruption of cell-cell contacts by EGTA, TNF and thrombin decreases Spry2 protein expression. In confluent cells, high Spry2 levels correlate with decreased extracellular signal-regulated kinase 1/2 (Erk1/2) phosphorylation. In contrast, dense Spry2 knockout MAECs exhibit enhanced signaling by Erk1/2. Moreover, inhibiting Erk1/2 activity in Spry2 knockout cells restores wild type cobblestone monolayer morphology. This study thus reveals a novel Spry2 function, which mediates endothelial contact inhibition and barrier integrity.

DOI: https://doi.org/10.1007/s10456-012-9330-9

Angiogenesis

Sprouty2 expression controls endothelial monolayer integrity and quiescence

--Manuscript Draft--

Manuscript Number:	AGEN-D-12-00608R2
Full Title:	Sprouty2 expression controls endothelial monolayer integrity and quiescence
Article Type:	Original Article
Keywords:	Sprouty2, endothelial quiescence, cell-cell contacts, FGF2, Erk1/2
Corresponding Author:	Rok Humar, PhD University Hospital Zürich Zurich, SWITZERLAND
Corresponding Author Secondary Information:	
Corresponding Author's Institution:	University Hospital Zürich
Corresponding Author's Secondary Institution:	
First Author:	Martin Anton Peier, MSc
First Author Secondary Information:	
Order of Authors:	Martin Anton Peier, MSc
	Thomas Walpen, MSc
	Gerhard Christofori, PhD
	Edouard J Battegay, M.D.
	Rok Humar, PhD
Order of Authors Secondary Information:	
Abstract:	Vascular integrity is fundamental to the formation of mature blood vessels and depends on a functional, quiescent endothelial monolayer. However, how endothelial cells enter and maintain quiescence in the presence of angiogenic factors is still poorly understood. Here we identify the fibroblast growth factor (FGF) antagonist Sprouty2 (Spry2) as a key player in mediating endothelial quiescence and barrier integrity in mouse aortic endothelial cells (MAECs): Spry2 knockout MAECs show spindle-like shapes and are incapable of forming a functional, impermeable endothelial monolayer in the presence of FGF2. Whereas dense wild type cells exhibit contact inhibition and stop to proliferate, Spry2 knockout MAECs remain responsive to FGF2 and continue to proliferate even at high cell densities. Importantly, the anti-proliferative effect of Spry2 is absent in sparsely plated cells. This cell density-dependent Spry2 function correlates with highly increased Spry2 expression in confluent wild type MAECs, while express Spry2. Spry2 protein expression is barely detectable in single cells but steadily increases in cells growing to high cell densities, with hypoxia being one contributing factor. At confluence, Spry2 expression correlates with intact cell-cell contacts, whereas disruption of cell-cell contacts by EGTA, TNF and thrombin decreases Spry2 protein expression. In confluent cells, high Spry2 levels correlate with decreased extracellular signal-regulated kinase 1/2 (Erk1/2) phosphorylation. In contrast, dense Spry2 knockout MAECs exhibit enhanced signaling by Erk1/2. Moreover, inhibiting Erk1/2 activity in Spry2 knockout cells restores wild type cobblestone monolayer morphology. This study thus reveals a novel Spry2 function, which mediates endothelial contact inhibition and barrier integrity.
Response to Reviewers:	Point-to-point response to reviewer's comments Reviewer 1 The authors have adequately responded to most concerns editorially. One additional set of experiments (Figure 5F,G) has been provided regarding the regulation of Spry2

	protein levels by cell-cell contact. The authors examine the effect of TNF or thrombin treatment on Spry2 protein expression by western blot and in parallel provide a electrical resistance profile, which reads out disruption of the cell-cell contacts by these agonists. There is a concern with the electrical resistance profiles (Figure 5G). First, it appears that the agonists were added before allowing the endothelial cells to establish a monolayer since there is a continual rise in resistance in control treated cells. Second, thrombin treatment usually leads to a drop but then a recovery of the resistance, unlike the prolonged disruption of barrier properties that are usually observed with TNF. This probably reflects the fact that the thrombin and TNF were added before cell-cell contacts were formed. These concerns should be addressed, as the objective of this set of experiments is to show that a disruption of the existing cell-cell contacts leads to a reduction in Spry2 protein levels. Our reply: We thank the reviewer for his evaluation and satisfaction about our clarifications for the major concerns and comments. Further we very much agree with the Reviewers justified concern about the electrical resistance profiles we provided. Indeed, we added TNF and Thrombin before cell contacts were formed. To resolve this issue we performed new experiments and added agonists after endothelial barrier stabilized. The results indeed show a rapid disruption of the endothelial barrier properties by thrombin with partial recovery as compared to a rather chronic destabilization by TNF. Furthermore, western blot analysis after 3 hours of agonist addition and barrier disruption confirmed Spry2 protein reduction for both TNF and thrombin. We thank the Reviewer for this thoughtful comment. The text and the Figure 5F,G including legend has been updated with these new experiments. Minor concern: Figure 5G is referred to as (F2) in the figure legend. Our reply: This issue has been resolved Reviewer 2: The authors have done a thorough job in addressing my comments and concerns. Our reply: Thank you very much.

Sprouty2 expression controls endothelial monolayer integrity and quiescence

Martin Peier[1], Thomas Walpen[1], Gerhard Christofori[2], Edouard Battegay[1,3], Rok Humar[1,3,*]

[1] Research Unit, Division of Internal Medicine, University Hospital Zurich, 8091 Zurich, Switzerland

[2] Department of Biomedicine, University of Basel, 4058 Basel, Switzerland

[3] Zurich Center for Integrative Human Physiology (ZIHP), Switzerland

[*] Corresponding author: Rok.Humar@usz.ch
University Hospital Zurich
Division Internal Medicine
Gloriastrasse 30, GLO30 J14
8091 Zurich
Switzerland
Tel: +41 (44) 634 5385
Fax: +41 (44) 634 5339

Running title: Sprouty2 and endothelial quiescence

Key words: Sprouty2, endothelial quiescence, cell-cell contacts, FGF2, Erk1/2

Summary

Vascular integrity is fundamental to the formation of mature blood vessels and depends on a functional, quiescent endothelial monolayer. However, how endothelial cells enter and maintain quiescence in the presence of angiogenic factors is still poorly understood. Here we identify the fibroblast growth factor (FGF) antagonist Sprouty2 (Spry2) as a key player in mediating endothelial quiescence and barrier integrity in mouse aortic endothelial cells (MAECs): Spry2 knockout MAECs show spindle-like shapes and are incapable of forming a functional, impermeable endothelial monolayer in the presence of FGF2. Whereas dense wild type cells exhibit contact inhibition and stop to proliferate, Spry2 knockout MAECs remain responsive to FGF2 and continue to proliferate even at high cell densities. Importantly, the anti-proliferative effect of Spry2 is absent in sparsely plated cells. This cell density-dependent Spry2 function correlates with highly increased Spry2 expression in confluent wild type MAECs, while express Spry2. Spry2 protein expression is barely detectable in single cells but steadily increases in cells growing to high cell densities, with hypoxia being one contributing factor. At confluence, Spry2 expression correlates with intact cell-cell contacts, whereas disruption of cell-cell contacts by EGTA, TNFα and thrombin decreases Spry2 protein expression. In confluent cells, high Spry2 levels correlate with decreased extracellular signal-regulated kinase 1/2 (Erk1/2) phosphorylation. In contrast, dense Spry2 knockout MAECs exhibit enhanced signaling by Erk1/2. Moreover, inhibiting Erk1/2 activity in Spry2 knockout cells restores wild type cobblestone monolayer morphology. This study thus reveals a novel Spry2 function, which mediates endothelial contact inhibition and barrier integrity.

Introduction

During angiogenesis a concerted action of hypoxia and growth factors including vascular endothelial growth factor (VEGF) and fibroblast growth factors (FGFs) induces the formation of endothelial tip cells and stalk cells, and promotes vascular cell proliferation, cell migration, and lumen formation [1-4]. Ultimately, these cells mature and stabilize into new, functional blood vessels that are able to control permeability and to supply the newly vascularized areas with oxygen and nutrients. In this physiological state, endothelial cells form a tight monolayer, resist apoptosis and remain quiescent (defined as reversible cell growth/proliferation arrest) even in the presence of angiogenic factors [5,6].

Endothelial cells in culture can display either an "activated" or a "quiescent" phenotype. The behavior of growing angiogenic (activated) cells is recapitulated by endothelial cells growing in sparse culture *in vitro* (thinly scattered cells), whereas a tight monolayer of cultured endothelial cells that is arranged in a cobblestone morphology is quiescent [5]. It has been suggested that several surface molecules associated with adherens and tight junctions mediate cell-contact inhibition (cells undergo growth arrest when they come into contact with each other) and vascular integrity through regulation of intracellular signaling cascades and transcription [7]. Endothelial cells mediate contact inhibition of growth in part by exiting cell cycle in response to the inhibition of extracellular signal-regulated kinase 1/2 (Erk1/2) activity, a major mitogen-activated kinase (MAPK) downstream of FGF and other angiogenic growth factors [8].

An important class of negative regulators of receptor tyrosine kinase (RTK) dependent MAPK activation is the Sprouty (Spry) family of proteins. In *Drosophila*, Sprouty (dSpry) modulates trachea branching [9] by inhibiting the RTK/Ras/Erk signaling downstream of different growth factors [10]. Sprouty2 (Spry2), one of four mammalian homologs, exhibits the highest sequence conservation across species [11] and plays a comparable role to dSpry in regulating the embryonic lung branching morphogenesis in mammals [12]. Furthermore, Spry2 modulates MAPK-signaling in embryogenesis [13,14], organ development [15], and angiogenesis in vivo and in vitro [16,17]. Spry2 is therefore a potential candidate to mediate cell-contact inhibition in endothelial cells.

Here, we have assessed the potential role of Spry2 in cell-contact inhibition and the formation and maintenance of the endothelial monolayer. We compared the ability of primary Spry2 expressing ($Spry2^{fl/fl}$) and Spry2 knockout ($Spry2^{-/-}$) mouse aortic endothelial cells (MAECs) to form a functional endothelial monolayer. Furthermore, we analyzed Spry2 expression and Erk1/2 activity in MAECs plated at defined cell densities. We were particularly interested of how endothelial cells process signals arising from increasing cell density to allow a switch from a proliferative, migratory phenotype to a quiescent, impermeable monolayer.

Materials and methods

Cell culture and treatments

Mouse aortic endothelial cells (MAECs) were isolated from aortae of C57BL/6 wild type male mice (MAECs ♂) or Sprouty2 floxed female mice (Spry2 floxed MAECs ♀) as described in a previous study (Humar et al., 2002). Cells were used for experiments up to passage 10. For all experiments in this study, cell culture dishes were coated with 0.1% gelatin (Carl Roth GmbH, Karlsruhe, Germany) for 20 minutes at 37°C. Cells were maintained in growth media (GM) [DMEM (Biochrom, Berlin, BW, Germany) complemented with 1% or 10% FCS, 1% sodium pyruvate, 1% non-essential amino acids, and 1% penicillin-streptomycin (Invitrogen, Carlsbad, CA, USA)] in a humidified 5% CO_2-air atmosphere at 37°C. Serumfree media (GM without FCS) was used for starvation. Cell numbers were assessed with a NucleoCounter® NC-100™ (Chemometec, Allerød, Denmark). MAECs were treated with one or more of the following growth factors and inhibitors: FGF2 25 ng/ml (R&D Systems, Minneapolis, MN, USA); MG132 5 μM and EGTA 2.5 mM (Merck, Billerica, MA, USA); Bapta-AM 10 μM (Invitrogen); TNFα 50 ng/ml (R&D Systems); thrombin 10 u/ml (Sigma-Aldrich, St. Louis, MO, USA), and U0126 5 μM (Promega, Madison, WI, USA). To create a hypoxic environment, cells were placed in a hypoxia incubator (Hera Cell 150) (Thermo Fisher Scientific, Waltham, MA, USA) with 1% oxygen for 24 hours. Micrograph pictures of cells were taken with a digital camera (F-viewXS) (Olympus, Hamburg, Germany) and an inverted microscope (1X71) (Olympus). GFP expression was monitored by using a U-LH100HG light source with a U-MWB2 filter (Olympus).

Generation of Spry2 knockout cells

We seeded 800,000 Spry2 floxed MAECs (♀) on a 10-cm culture dish. The next day, the media was removed and a virus (100 MOI) that contained either Ade-CRE-GFP or Ade-CMV-GFP (Vector Biolabs, Philadelphia, PA, USA) was added in 3 ml of growth media to the cells. After 6 hours, the media was removed, replaced by 10 ml of normal growth media, and then incubated at 37°C. Endothelial cells expressed GFP the following day. Down-regulation of Spry2 was assessed by using qRT-PCR and Western blot. Steps that involved handling viruses or virus-transfected cells were undertaken in a level-2 biosafety hood (VSB 90) (Skan, Allschwil, Basel, Switzerland) in a certified cell culture laboratory.

mRNA extraction and quantitative real-time PCR

To isolate RNA from cells, cells were first harvested by scraping with a cell scraper (BD) and the RNA then isolated by using RNeasy kit (Qiagen, Hilden, NRW, Germany) according to directions in the manufacturer's manual. The RNA was then reverse transcribed to cDNA by using the Taqman Kit (Applied Biosystems, Foster City, CA, USA). The following primers were used for qRT-PCR: Spry2-fwd (ATAATCCGAGTGCAGCCTAAATC), Spry2-rev (CGCAGTCCTCACACCTGTAG), GAPDH-fwd (TGTGTCCGTCGTGGATCTGA), and GAPDH-rev (CCTGCTTCACCACCTTCTTGA). The cDNA samples and the forward and reverse primers for the endogenous control gene (GAPDH) and the target gene (Spry2), together with SYBR green PCR master mix (Applied Biosystems) were loaded on a 96-well PCR reaction plate.

Data was collected and normalized to GAPDH by running the relative quantitation program with the 7500 real time PCR system (Applied Biosystems).

Immunoblotting

To extract protein from the cells, cells were washed twice with ice-cold PBS and then harvested by scraping with a cell scraper (BD, Franklin Lakes, NJ, USA) into1 ml of ice-cold PBS. The cell suspension was collected and then centrifuged for 5 minutes at 14,000 rpm at 4°C. The pellet was re-suspended in RIPA buffer that contained a complete mini protease inhibitor (Roche, Basel, Switzerland) and a phosphatase inhibitor cocktail 2 (Sigma-Aldrich) and then was lysed by using liquid nitrogen in four freeze-and-thaw cycles. The sample was centrifuged for 15 minutes at 14,000 rpm at 4°C. The resulting supernatant was collected and the protein concentration measured by using a BCA protein assay kit (Thermo Fisher Scientific). Equal amounts of protein were separated by SDS-PAGE and then transferred to a nitrocellulose membrane (BA85) (Whatman, Maidstone, Kent, UK) by using a semidry blotting procedure. Membranes were blocked for 1 hour at room temperature (RT) in TBS that contained 5% skim milk powder (Sigma-Aldrich), washed once with TBS that contained 0.1% tween (TBST) and then incubated overnight at 4°C with one of the following primary antibodies: rabbit anti Sprouty2 (H-120) 1:4,000 (Santa Cruz Biotechnology, Santa Cruz, CA, USA); rabbit anti Sprouty2 (ab50317) 1:1,000 (Abcam, Cambridge, Cambs, UK); rabbit anti pospho-Erk1/2 (9102) 1:1,000, and rabbit anti total-Erk1/2 (9102) 1:1,000 (Cell Signaling, Danvers, MA, USA); rabbit anti Hif-1α (NB100-479) 1:1,000 (Novus Biologicals, Littleton, CO, USA); and mouse anti β-Actin 1:10,000 (A-5441) (Sigma-Aldrich).
The next day, the membrane was washed three times in TBST and incubated with a secondary antibody—goat anti rabbit antibody HRP (7074) 1:5,000 – 1:20,000 (Cell Signaling) or anti mouse HRP (7076) (1:80,000) (Cell Signaling)—for 1 hour at RT. After another wash step, a chemiluminescent substrate that is used for the detection of HRP (Thermo Fisher Scientific) was applied to the membrane for 1 minute. The signal was detected with CL-XPosure film (Thermo Fisher Scientific), and the resulting bands were quantified by using ImageJ (Wayne Rasband, NIH, MD, USA).

Proliferation Assay

Spry2 KO and Spry2 wilt type MAECs (♀) were seeded at the indicated densities in 8 replicates and grown in 100 µl of growth media with 1% FCS in a 96-well plate both with and without 25 ng/ml of FGF2. After 48 hours, 10 µl of alamarBlue® solution (Invitrogen) was added for 3 hours. Fluorescence was measured (Ex 560; Em 590) by using a Spectramax M2 reader (Molecular Devices, Sunnyvale, CA, USA).

Permeability assay

The permeability assay was performed according to directions in the manufacturer's manual (Millipore, Billerica, MA, USA). 200,000 Spry2 KO and Spry2 wild type MAECs (♀) were suspended in 200 µl of complete growth medium supplemented with 1% FCS and both with and without 25 ng/ml of FGF2. The cells were then seeded in triplicate on cell culture inserts (3-µm pore size) (Millipore) and placed in 24-well culture plates (BD) that contained 600 µl of FGF2-free medium per well. After 48 hours, the inserts were moved to a

new 24-well plate and 70 kDa FITC-dextran was added for 10 minutes. Fluorescence at Ex 585 nm and Em 520 nm of the lower well compartments was analyzed by using a Spectramax M2 reader.

Oxygen sensing

Changes in the oxygen saturation of cell cultures were measured in real time by using an SDR SensorDish reader (Presens, Regensburg, BY, Germany). MAECs (♂) were plated on an Oxodish 24-well plate (OD24) with integrated oxygen sensors (Presens). Oxygen saturation of the media was measured every 30 minutes and data was collected and analyzed by using SDR_v38 software (Presens) on a personal computer.

Electric cell-substrate impedance sensing (ECIS)

Electrical resistance measurements were performed using an ECIS ZΘ apparatus (Applied Biopyhysics, Troy, NY, USA) in 8-well (0.8 cm^2/well) arrays with 40 (8W10E+) gold electrodes, each with a diameter of 250 μm (Applied Biopyhysics). Each experiment was carried out in duplicate. Before seeding the cells, each well was pre-incubated with serum-free DMEM overnight that was followed by a 20 minute coating with 0.1% gelatin (Carl Roth GmbH) and 0.9% sodium chloride in PBS followed by three wash steps with growth media. The arrays in the measurement station were then placed in an incubator (37°C, 5% CO_2) to allow real time monitoring. Total resistance was measured at a frequency of 4 kHz. Initial baseline values were normalized to 1.

Statistical analysis

All statistical tests were performed by using GraphPad Prism 5.04 for Windows® (GraphPad software, San Diego, CA, USA). We use unpaired t-test to evaluate differences between two groups. If there were more than two groups, we used one-way ANOVA, followed by a Newman-Keuls post-test. $P<0.05$ was considered significant.

Results

Lack of Spry2 expression results in loss of contact inhibition and endothelial monolayer integrity

We generated Spry2 knockout MAECs (mouse aortic endothelial cells) to explore whether Spry2 regulates the formation of the endothelial monolayer and thereby mediates cell-contact inhibition. Adenoviral transfection of floxed-Spry2 MAECs with a Cre recombinase encoding expression vector (Ade-CRE-GFP), but not with a control vector (Ade-CMV-GFP), efficiently down-regulated Spry2 mRNA and protein levels (Fig. 1A-D).
$Spry2^{-/-}$ (knockout) and $Spry2^{fl/fl}$ (wild type) MAECs were then seeded at confluence in the presence or absence of FGF2. We observed that $Spry2^{-/-}$ MAECs grown for 48 hours in the presence of FGF2, were incapable of forming a mature monolayer and displayed an elongated, angiogenic phenotype with longitudinal gaps between the cells and little cell-cell contacts (Fig. 2A2). In contrast to the latter results, control $Spry2^{fl/fl}$ MAECs formed a regular cobblestone-type cell monolayer with only a few elongated cells (Fig. 2A1). FGF2 was required to disturb layer formation in $Spry2^{-/-}$ MAECs, because without FGF2 stimulation, $Spry2^{-/-}$ and $Spry2^{fl/fl}$ cells both formed a regular mature monolayer (Fig. 2A1,A2).
To further characterize the perturbed endothelial monolayer formation by $Spry2^{-/-}$ cells, we analyzed monolayer permeability. Indeed, the monolayer formed by $Spry2^{-/-}$ cells exhibited significantly increased permeability to a 70 kDa FITC-dextran in the presence of FGF2, while no difference was observed in cells without FGF2 (Fig. 2B). $Spry2^{-/-}$ MAECs appear to fail in establishing cell contact inhibition. We therefore asked, whether $Spry2^{-/-}$ cells show increased cell proliferation. We then plated the cells at different densities and let them grow for 48 h in the presence or absence of FGF2 before evaluating the cell cumbers. No difference was observed between $Spry2^{-/-}$ and $Spry2^{fl/fl}$ when cells were plated at initially sparse conditions (3,000 cells/cm^2) (Fig. C1). However, when the cells were plated with a higher initial density (6,000 and 12,000 cells/cm^2), the cell numbers increased significantly in $Spry2^{-/-}$ MAECs as compared to $Spry2^{fl/fl}$ MAECs after 48 hours of FGF2 stimulation (Fig. C2, C3). No difference was observed between $Spry2^{-/-}$ and $Spry2^{fl/fl}$ when cells were grown without FGF2. These findings indicate that Spry2 is indispensable for endothelial cell monolayer formation and the maintenance of barrier integrity in the presence of FGF2. Apparently, the function of Spry2 thereby depends on an increased cell density.

High cell density induces Spry2 expression

Next we asked, whether the Spry2 function at high cell densities correlated with increased Spry2 expression at high cell densities. We therefore compared Spry2 protein expression of cells, which were seeded at different densities (Fig. 3A). Sparsely plated cells (1,500 – 6,000 cells/cm^2) expressed Spry2 protein at very low levels. Subconfluently plated cells (12,000 – 25,000 cells/cm^2) increased Spry2 protein markedly. Plating 50,000 cells/cm^2 led to the formation of a confluent monolayer and a strong induction Spry2 protein (Fig. 3B). We then analyzed the Spry2 mRNA expression of sparse (3,000 cells/cm^2) and confluent cells (50,000 cells/cm^2) and compared it to the corresponding protein expression. Whereas the Spry2 protein levels increased 70 fold in confluent compared to sparse cells, the mRNA levels increased only moderately (two fold), suggesting that density dependent Spry2 expression is regulated predominantly at a post transcriptional level.

To better understand the fashion of cell density-induced Spry2 expression, we analyzed Spry2 protein expression during formation of the endothelial monolayer. MAECs were plated sparsely and grown to high cell density and confluence over a time period of 24 to 96 hours (Fig. 4A). Spry2 expression increased markedly after 48 hours, and reached its maximum level between 72 and 96 hours after seeding (Fig. 4B). Thus, Spry2 protein expression increased not only when cells were plated at high cell density, but also when cells grow from an initial sparse culture to a confluent culture.

Hypoxia increases Spry2 expression during formation of the endothelial monolayer

Conventional monolayer cultures are often hypoxic when incubated in an air/5% CO_2 atmosphere [18]. Thus, hypoxia that results from increased oxygen-consumption during endothelial monolayer formation may correlate with high cell density and may upregulate Spry2 expression. To investigate this hypothesis, we analyzed the expression of the hypoxia marker Hif-1α over a time period of 24 to 96 hours. Hif-1α levels increased at 48 hours, dropped at 72 hours, and were undetectable after 96 hours of cell seeding (Fig. 4A). We then further substantiated these findings by measuring oxygen levels of sparsely seeded cells directly and in real time over a period of 0-96 hours: Oxygen saturation decreased slightly after 24 hours (80% $O_{2\ saturation}$) and declined to a minimum between 48 and 72 hours after cell seeding (70% $O_{2\ saturation}$) compared to a control with no cells present (85% $O_{2\ saturation}$ throughout the experiment) (Fig. 4B). These results demonstrate that increased Spry2 expression after 48 hours of endothelial cells growing to confluence is accompanied by hypoxia and elevated Hif-1α expression.

To investigate whether hypoxia indeed induces Spry2 protein expression, we reduced oxygen consumption by starving the cells to reduce metabolism [18]. Indeed, Spry2 protein levels decreased but were still detectable in starved cells (Fig. 4C). In addition, Hif-1α protein levels dropped and were undetectable after changing growth media to serum-free conditions (Fig. 4C). In parallel experiments replacement of the growth media by serum-free media after 24 hours reduced the oxygen consumption of the endothelial cell cultures and restored basal oxygen levels after 48 hours. However, in the presence of serum, oxygen levels decreased further and reached a minimum level (65% $O_{2\ saturation}$) after 48 hours of cell seeding (Fig. 4D).

To assess whether endothelial cells cultured in serum-free medium did not lose the potential to induce Spry2 expression under hypoxia, cells were seeded at sparse or confluent density, and serum-free endothelial cells were subjected to hypoxic (1% O_2) and normoxic conditions in a hypoxia incubator. After 24 hours, Spry2 increased in cells under hypoxic conditions; this correlated with increased Hif-1α protein levels (Fig. 4E). Hypoxia, however, did not affect Spry2 mRNA levels (Fig. 4F). Thus, it is likely that hypoxia regulates Spry2 expression independent of Hif-1α on a post-transcriptional level.

Disruption of calcium dependent cell-cell contacts decreases Spry2 protein in confluent cells

Although transient hypoxia induced Spry2 expression in the early phase of endothelial cell monolayer formation, it appeared that hypoxia was not necessary to maintain high Spry2 levels when the cells reached confluence (Figs. 3B). Therefore, we hypothesized that in confluent cells Spry2 might be stabilized at an elevated level through a hypoxia-independent mechanism, including cell-cell contact.

To examine whether cell-cell contact regulates Spry2, we used ethylene glycol tetraacetic acid (EGTA) to chelate extracellular calcium and to disrupt calcium-dependent cell-cell contacts [19]. The addition of EGTA to confluent MAECs resulted in the formation of gaps between cells after 30 minutes and in a complete detachment from each other after 3 hours (Fig. 5A). Replacement of EGTA with new media restored the monolayer after 24 hours of incubation. In parallel experiments, treatment with EGTA completely eliminated Spry2 expression after 0.5 and 3 hours of EGTA treatment (Fig. 5B). The restoration of the monolayer by new media also restored Spry2 protein to the levels seen prior to EGTA treatment. In addition, we measured the electrical resistance of the confluent endothelial monolayer during EGTA treatment by electrical cell impedance sensing (ECIS). The electrical resistance dropped markedly after the addition of EGTA and then returned to basal levels (resistance prior the addition of EGTA) within 48 hours after the addition of new media. This result demonstrated that the effect of treatment with EGTA was reversible and did not damage endothelial cell viability (Fig. 5C). Of note, chelation of intracellular calcium with Bapta-AM did not affect Spry2 protein levels (Fig. 5D), and neither EGTA nor Bapta-AM affected Spry2 mRNA levels (Fig. 5E).

Our results indicate that high Spry2 protein levels restrict endothelial permeability in confluent cells. Since several physiologic conditions such as inflammation display and require increased monolayer permeability, we asked whether Spry2 protein expression can be decreased by physiological mediators of endothelial permeability such as TNFα [20,21] and thrombin [22]. Indeed, Spry2 protein expression decreased when confluent cells were treated for 3 hours with either TNFα or thrombin as compared to the control cells (Fig. 5F). As control for the increased permeability, we measured the change in total resistance of cells after addition of either TNFα or thrombin. As expected, the results showed a rapid disruption of the endothelial barrier properties by thrombin with partial recovery as compared to a rather chronic destabilization by TNFα (Fig. 5G). Taken together, these findings demonstrate that density-dependent Spry2 protein expression depends on intact cell-cell contacts and is downregulated by agents that increases endothelial permeability.

At high cell densities high Spry2 protein levels correlate with decreased Erk1/2 phosphorylation

A well-established inhibitor of Erk1/2 activity downstream of FGF signaling [23,17] Spry2 might mediate cell-contact inhibition in confluent cells via Erk1/2 inhibition. We therefore compared Spry2 expression with Erk1/2 phosphorylation in sparse and confluent cells. In sparse cells, FGF2-induced Erk1/2 phosphorylation levels were detected along with low Spry2 protein levels (Fig. 3C). Vice versa, Spry2 was exclusively increased in confluent cells and correlated with decreased Erk1/2 phosphorylation. In the presence of FGF2, cell confluence significantly decreased FGF2-induced Erk1/2 phosphorylation when compared to sparse, FGF2-stimulated cells (Fig. 3C). Taken together, these results suggest that cell density is crucial to regulate Spry2 expression and by that its function as an inhibitor of FGF2-Erk1/2 signaling.

Inhibition of Erk1/2 signaling restores wild type morphology of the monolayer

Next we asked, whether $Spry^{-/-}$ MAECs exhibited increased Erk1/2 phosphorylation. Indeed, in $Spry2^{-/-}$ cells, FGF2-induced Erk1/2 phosphorylation levels increased 2.5 fold compared to those in $Spry2^{fl/fl}$ cells, while Erk1/2 phosphorylation was absent without stimuli in both cell types (Fig. 2A1,A2).

We therefore investigated whether inhibiting the MAPK Erk1/2 pathway could reverse disturbed endothelial monolayer formation of Spry2$^{-/-}$ cells. Spry2$^{fl/fl}$ and Spry2$^{-/-}$ MAECs were plated in the presence or absence of the Erk1/2 inhibitor U0126. In the absence of U0126, Spry2$^{-/-}$ MAECs showed a highly angiogenic phenotype upon FGF2 stimulation. However, when cells were pre-incubated with U0126 before adding FGF2, the wild type cobblestone phenotype was restored (Fig. 2B). The absence of Erk1/2 phosphorylation upon U0126-treatment in both Spry2$^{fl/fl}$ and Spry2$^{-/-}$ MAECs demonstrated the efficacy of the Erk1/2 inhibitor (Fig. 2C). Notably, upon inhibition of Erk1/2 Spry2 expression was reduced in Spry2$^{fl/fl}$ cells, indicating that the expression of Spry2 is partly regulated by Erk1/2 signaling. These findings show that Spry2, as a regulator of Erk1/2 activity, is indispensable for endothelial cell monolayer formation and the maintenance of barrier integrity in the presence of FGF2.

Discussion

Cell-contact inhibition is an important process for the regulation of vascular integrity for which proper understanding underlying molecular events is still lacking. This study therefore addresses the important question of how endothelial cells process signals arising from increasing cell density to allow a switch from a proliferative, migratory phenotype to a quiescent, impermeable monolayer. Here, we identify the FGF receptor signaling antagonist Spry2 as a key component in the establishment of endothelial quiescence and barrier integrity.

Spry2 exclusively acts as an adaptor protein without any enzymatic activity [24]. Therefore cells have restricted possibilities to control Spry2 function: by regulating its abundance [25-27], its localization [17,28], and/or its post-transcriptional modifications [29-31]. Here we show, that in primary endothelial cells, Spry2 is regulated in a previously unknown cell-density dependent fashion and is found at high levels only in dense endothelial cell monolayers. Highly elevated Spry2 protein levels might inhibit endothelial proliferation and, thus, maintain vascular integrity and quiescence. Forced Spry2 expression in human umbilical vein endothelial cells was shown to inhibit growth factor-induced proliferation and sprouting [17]. We here demonstrate that sparse cultures of proliferating endothelial cells express low Spry2 protein levels and that upon reaching cell confluence and cell quiescence Spry2 protein levels increase by a mostly post-transcriptional mechanism. Notably, ablation of Spry2 in dense cells increases cell proliferation and permeability of the endothelial monolayer. Thus restriction of Spry2 may allow endothelial cell proliferation and migration during angiogenesis and wound closure [32,16]. In accord with our findings, Zhang et al. showed that Spry2 protein decreased in the vasculature after an injury to the endothelial lining of the carotid artery in rats and then reappeared weeks later after the inner endothelial lining had re-formed [33]. We report that Spry2 protein levels increase steadily in cells that are growing toward confluence. Two independent and consecutive stimuli induce and stabilize Spry2 protein levels – transient intrinsic hypoxia and the establishment of cell-cell contacts. In the sub-confluent phase, Spry2 expression correlates with reduced oxygen saturation and increases Hif-1α protein levels. Furthermore, exogenously applied hypoxia increases Spry2 protein in both sparse (results not shown) and confluent cells in post transcriptional manner. A possible explanation for this finding is delivered by Anderson et al [25]. They showed that Spry2 interacts with prolyl hydroxylases preferentially during normoxic conditions. When hydroxylated on proline residues, Spry2 is recognized by pVHL and its associated E3 ubiquitin ligase complex, resulting in Spry2 degradation. Thus under hypoxic conditions, when PDHs are less active, Spry2 levels increase [25].

In vivo, hypoxia-induced Spry2 expression may provide a protective homeostatic function when the vasculature is exposed to hypoxia. Endothelium that is subjected to oxygen deprivation maintains cell viability and basic biosynthetic mechanisms, but it displays multiple changes in barrier function that are relevant to vascular homeostasis [34,35].

The observation that Spry2 expression still remains elevated in confluent cells showing normoxic oxygen levels points to another essential mechanism for stabilizing Spry2 in confluent cultures: intact cell-cell contacts. An intriguing question is how Spry2 is induced when cells reach confluence. Possible membrane initiators of the intracellular signals engaged by direct cell-to-cell contacts are the N- and VE-cadherins. N- and VE-cadherins are components of endothelial adherens junctions [36,37] and interact with cadherins of neighboring cells in a homophilic manner [38]. These adhesive complexes strictly depend on extracellular calcium [19,39]. We show that Ca^{2+} depletion disrupts cell-cell contacts and rapidly destabilizes Spry2 protein. Conversely, the formation

of cell-cell contacts stabilizes Spry2 protein even at a stage, at which an impermeable endothelial barrier is not yet completely re-established. Thus, singular cell-cell contacts may already suffice to stabilize Spry2 protein levels. Consistent with this notion, previous reports have indicated that cadherin clustering induces signaling, and these events may stabilize Spry2 levels, when cells first touch each other before complete confluence is reached and junctions are fully stabilized [40,41]. Thus, our findings point to calcium dependent cell-cell interactions which are needed for Spry2 expression when cells grow to confluence, with the final evidence of proof still to be elucidated in future. The observation that TNFα and thrombin increase endothelial permeability and at the same time, decrease Spry2 expression further add to the assumption that cell-cell contact upregulate Spry2 protein expression. In situations such as inflammation, the endothelial permeability needs to be increased to allow transmigration of immune cells to fight pathogens [42]. Since high Spry2 levels correlate with decreased endothelial permeability, cells might be forced to restrict Spry2 expression in confluent cells via physiological agonists of endothelial permeability such as TNFα and thrombin [20-22].

At high cell density, cell-cell contact inhibition promotes the switch from an angiogenic and proliferative state to a quiescent endothelial cell phenotype. It is assumed that membrane proteins in addition to maintaining cell-cell adhesion, also sense cell-cell interactions and transduce this information to intracellular signaling cascades [5,43]. In endothelial cells for example, contact inhibition is mediated in part through inhibition of Erk1/2 [8]. Spry2 is a well-known feed-back loop inhibitor of RTK signaling and modulates Erk1/2 activity in various settings [16]. Therefore, we have hypothesized that Spry2, by inhibiting Erk1/2 activity, promotes cell contact inhibition in confluent endothelial cells. Indeed, Spry2 expression correlates with decreased Erk1/2 activity at high cell density. Vice versa, ablation of Spry2 in confluent cells increases FGF2-induced but not basal Erk1/2 signaling. As a result, Spry2$^{-/-}$ cells fail to form a connected monolayer and exhibit a spindle-shaped morphology with increased proliferation and monolayer permeability in the presence of FGF2.

The inability of Spry2$^{-/-}$ cells to form a functional monolayer is likely due to unrestricted FGF2-Erk1/2 signaling because Erk1/2 inhibition in Spry2$^{-/-}$ cells restores the wild type-like endothelial cobblestone phenotype. We speculate that unrestricted FGF2-Erk1/2 signaling activates Hif-1α-induced gene regulation: experimental evidence in several studies has demonstrated that FGF2 activates the VEGF/VEGFR system [44,45] in part via Hif-1α [46-48]. Whereas fine-tuned intracellular VEGF-A/VEGFR-2 signaling supports endothelial survival in established mature blood vessels [49], uncontrolled expression of VEGF-A exceeding physiological thresholds leads to the formation of unstable and leaky blood vessels [50] or even hemangiomas [51]. Spry2 could potentially interfere with this signaling cascade and prevent activation of the VEGF/VEGFR system by FGF in quiescent blood vessels.

Spry2 knockout animals display discrete developmental defects that have been attributed to unrestricted FGF signaling [52-55]. Although we observe that Spry2 knockout markedly affected endothelial quiescence and integrity *in vitro*, Spry2 knockout mice seem to exhibit rather mild malformations without an overt vascular phenotype. This discrepancy might be due to redundancies amongst the Sprouty isoforms in *in vivo* models. Furthermore, exposition of the knockout animals to stress, such as severe hypoxia or high doses of growth factors, might reveal additional Spry2-specific phenotypes.

FGF signaling has been identified as a strong pro-angiogenic factor in physiological [4] and pathological situations [56]. Murakami et al. [57] have demonstrated, however, that it also plays a key role in the maintenance of vascular integrity, because disrupted FGF signaling results in severe impairment of the endothelial barrier function and eventually to a disintegration of the vasculature. Therefore, we propose that Spry2, by controlling

Erk1/2 signaling, switches the response of endothelial cells to FGF2 from proliferation and migration to survival and quiescence (Fig. 7).

In conclusion, the data of the present study show for the first time that high Spry2 expression levels play a critical role in endothelial monolayer formation and stabilization by inhibiting FGF2-induced Erk1/2 signaling. This negative feedback loop may be important in situations, where endothelial monolayers form, where the regulation of basal permeability must be strict, and where vascular integrity and quiescence must be established and maintained *in vivo*. For example, endothelial Spry2 expression might prevent damage to the blood–brain barrier and the development of vasogenic brain edema under prolonged hypoxia at high altitude [58] or may promote vessel normalization by inhibiting extensive growth-factor signaling in cancer [59].

.

Acknowledgements We thank O. Sansom and I. Ahmad, who kindly provided the Floxed-Spry2 mouse strains (Beatson Institute, Glasgow, Scotland). We are grateful to M. A. Cabrita and I. Bhattacharya for helpful discussions. We thank Sigrid Strom, Ina Kalus and Elvira Haas for critical review of the manuscript. This work was supported by grants from the Swiss National Science Foundation to E. J. B. and from the University of Zürich.

Conflict of interest The authors declare no conflict of interest.

References

1. Carmeliet P (2005) Angiogenesis in life, disease and medicine. Nature 438 (7070):932-936. doi:nature04478 [pii]
10.1038/nature04478
2. Adams RH, Alitalo K (2007) Molecular regulation of angiogenesis and lymphangiogenesis. Nat Rev Mol Cell Biol 8 (6):464-478. doi:nrm2183 [pii]
10.1038/nrm2183
3. De Smet F, Segura I, De Bock K, Hohensinner PJ, Carmeliet P (2009) Mechanisms of vessel branching: filopodia on endothelial tip cells lead the way. Arterioscler Thromb Vasc Biol 29 (5):639-649. doi:ATVBAHA.109.185165 [pii]
10.1161/ATVBAHA.109.185165
4. Presta M, Dell'Era P, Mitola S, Moroni E, Ronca R, Rusnati M (2005) Fibroblast growth factor/fibroblast growth factor receptor system in angiogenesis. Cytokine Growth Factor Rev 16 (2):159-178. doi:S1359-6101(05)00005-5 [pii]
10.1016/j.cytogfr.2005.01.004
5. Dejana E (2004) Endothelial cell-cell junctions: happy together. Nat Rev Mol Cell Biol 5 (4):261-270. doi:10.1038/nrm1357
nrm1357 [pii]
6. Murakami M, Simons M (2009) Regulation of vascular integrity. J Mol Med (Berl) 87 (6):571-582. doi:10.1007/s00109-009-0463-2
7. Dejana E, Tournier-Lasserve E, Weinstein BM (2009) The control of vascular integrity by endothelial cell junctions: molecular basis and pathological implications. Dev Cell 16 (2):209-221. doi:S1534-5807(09)00032-X [pii]
10.1016/j.devcel.2009.01.004
8. Vinals F, Pouyssegur J (1999) Confluence of vascular endothelial cells induces cell cycle exit by inhibiting p42/p44 mitogen-activated protein kinase activity. Mol Cell Biol 19 (4):2763-2772
9. Hacohen N, Kramer S, Sutherland D, Hiromi Y, Krasnow MA (1998) sprouty encodes a novel antagonist of FGF signaling that patterns apical branching of the Drosophila airways. Cell 92 (2):253-263. doi:S0092-8674(00)80919-8 [pii]
10. Casci T, Vinos J, Freeman M (1999) Sprouty, an intracellular inhibitor of Ras signaling. Cell 96 (5):655-665. doi:S0092-8674(00)80576-0 [pii]
11. Minowada G, Jarvis LA, Chi CL, Neubuser A, Sun X, Hacohen N, Krasnow MA, Martin GR (1999) Vertebrate Sprouty genes are induced by FGF signaling and can cause chondrodysplasia when overexpressed. Development 126 (20):4465-4475
12. Tefft JD, Lee M, Smith S, Leinwand M, Zhao J, Bringas P, Jr., Crowe DL, Warburton D (1999) Conserved function of mSpry-2, a murine homolog of Drosophila sprouty, which negatively modulates respiratory organogenesis. Curr Biol 9 (4):219-222. doi:S0960-9822(99)80094-3 [pii]
13. Mailleux AA, Tefft D, Ndiaye D, Itoh N, Thiery JP, Warburton D, Bellusci S (2001) Evidence that SPROUTY2 functions as an inhibitor of mouse embryonic lung growth and morphogenesis. Mech Dev 102 (1-2):81-94. doi:S0925477301002866 [pii]

14. Taniguchi K, Ayada T, Ichiyama K, Kohno R, Yonemitsu Y, Minami Y, Kikuchi A, Maehara Y, Yoshimura A (2007) Sprouty2 and Sprouty4 are essential for embryonic morphogenesis and regulation of FGF signaling. Biochem Biophys Res Commun 352 (4):896-902. doi:S0006-291X(06)02593-9 [pii] 10.1016/j.bbrc.2006.11.107
15. Mason JM, Morrison DJ, Basson MA, Licht JD (2006) Sprouty proteins: multifaceted negative-feedback regulators of receptor tyrosine kinase signaling. Trends Cell Biol 16 (1):45-54. doi:S0962-8924(05)00299-0 [pii] 10.1016/j.tcb.2005.11.004
16. Cabrita MA, Christofori G (2008) Sprouty proteins, masterminds of receptor tyrosine kinase signaling. Angiogenesis 11 (1):53-62. doi:10.1007/s10456-008-9089-1
17. Impagnatiello MA, Weitzer S, Gannon G, Compagni A, Cotten M, Christofori G (2001) Mammalian sprouty-1 and -2 are membrane-anchored phosphoprotein inhibitors of growth factor signaling in endothelial cells. J Cell Biol 152 (5):1087-1098
18. Metzen E, Wolff M, Fandrey J, Jelkmann W (1995) Pericellular PO2 and O2 consumption in monolayer cell cultures. Respir Physiol 100 (2):101-106. doi:003456879400125J [pii]
19. Schnittler HJ, Puschel B, Drenckhahn D (1997) Role of cadherins and plakoglobin in interendothelial adhesion under resting conditions and shear stress. Am J Physiol 273 (5 Pt 2):H2396-2405
20. Goldblum SE, Hennig B, Jay M, Yoneda K, McClain CJ (1989) Tumor necrosis factor alpha-induced pulmonary vascular endothelial injury. Infect Immun 57 (4):1218-1226
21. McKenzie JA, Ridley AJ (2007) Roles of Rho/ROCK and MLCK in TNF-alpha-induced changes in endothelial morphology and permeability. J Cell Physiol 213 (1):221-228. doi:10.1002/jcp.21114
22. Lum H, Del Vecchio PJ, Schneider AS, Goligorsky MS, Malik AB (1989) Calcium dependence of the thrombin-induced increase in endothelial albumin permeability. J Appl Physiol 66 (3):1471-1476
23. Gross I, Bassit B, Benezra M, Licht JD (2001) Mammalian sprouty proteins inhibit cell growth and differentiation by preventing ras activation. J Biol Chem 276 (49):46460-46468. doi:10.1074/jbc.M108234200 M108234200 [pii]
24. Guy GR, Jackson RA, Yusoff P, Chow SY (2009) Sprouty proteins: modified modulators, matchmakers or missing links? J Endocrinol 203 (2):191-202. doi:JOE-09-0110 [pii] 10.1677/JOE-09-0110
25. Anderson K, Nordquist KA, Gao X, Hicks KC, Zhai B, Gygi SP, Patel TB (2011) Regulation of cellular levels of Sprouty2 protein by prolyl hydroxylase domain and von Hippel-Lindau proteins. J Biol Chem 286 (49):42027-42036. doi:M111.303222 [pii] 10.1074/jbc.M111.303222
26. Ding W, Shi W, Bellusci S, Groffen J, Heisterkamp N, Minoo P, Warburton D (2007) Sprouty2 downregulation plays a pivotal role in mediating crosstalk between TGF-beta1 signaling and EGF as well as FGF receptor tyrosine kinase-ERK pathways in mesenchymal cells. J Cell Physiol 212 (3):796-806. doi:10.1002/jcp.21078
27. Ding W, Warburton D (2008) Down-regulation of Sprouty2 via p38 MAPK plays a key role in the induction of cellular apoptosis by tumor necrosis factor-alpha. Biochem Biophys Res Commun 375 (3):460-464. doi:S0006-291X(08)01581-7 [pii] 10.1016/j.bbrc.2008.08.037

28. Lim J, Wong ES, Ong SH, Yusoff P, Low BC, Guy GR (2000) Sprouty proteins are targeted to membrane ruffles upon growth factor receptor tyrosine kinase activation. Identification of a novel translocation domain. J Biol Chem 275 (42):32837-32845. doi:10.1074/jbc.M002156200
M002156200 [pii]
29. Fong CW, Leong HF, Wong ES, Lim J, Yusoff P, Guy GR (2003) Tyrosine phosphorylation of Sprouty2 enhances its interaction with c-Cbl and is crucial for its function. J Biol Chem 278 (35):33456-33464. doi:10.1074/jbc.M301317200
M301317200 [pii]
30. Hanafusa H, Torii S, Yasunaga T, Nishida E (2002) Sprouty1 and Sprouty2 provide a control mechanism for the Ras/MAPK signalling pathway. Nat Cell Biol 4 (11):850-858. doi:10.1038/ncb867
ncb867 [pii]
31. Mason JM, Morrison DJ, Bassit B, Dimri M, Band H, Licht JD, Gross I (2004) Tyrosine phosphorylation of Sprouty proteins regulates their ability to inhibit growth factor signaling: a dual feedback loop. Mol Biol Cell 15 (5):2176-2188. doi:10.1091/mbc.E03-07-0503
E03-07-0503 [pii]
32. Glienke J, Schmitt AO, Pilarsky C, Hinzmann B, Weiss B, Rosenthal A, Thierauch KH (2000) Differential gene expression by endothelial cells in distinct angiogenic states. Eur J Biochem 267 (9):2820-2830. doi:ejb1325 [pii]
33. Zhang C, Chaturvedi D, Jaggar L, Magnuson D, Lee JM, Patel TB (2005) Regulation of vascular smooth muscle cell proliferation and migration by human sprouty 2. Arterioscler Thromb Vasc Biol 25 (3):533-538. doi:01.ATV.0000155461.50450.5a [pii]
10.1161/01.ATV.0000155461.50450.5a
34. Pinsky DJ, Yan SF, Lawson C, Naka Y, Chen JX, Connolly ES, Jr., Stern DM (1995) Hypoxia and modification of the endothelium: implications for regulation of vascular homeostatic properties. Semin Cell Biol 6 (5):283-294
35. Yan SF, Ogawa S, Stern DM, Pinsky DJ (1997) Hypoxia-induced modulation of endothelial cell properties: regulation of barrier function and expression of interleukin-6. Kidney Int 51 (2):419-425
36. Lampugnani MG, Corada M, Caveda L, Breviario F, Ayalon O, Geiger B, Dejana E (1995) The molecular organization of endothelial cell to cell junctions: differential association of plakoglobin, beta-catenin, and alpha-catenin with vascular endothelial cadherin (VE-cadherin). J Cell Biol 129 (1):203-217
37. Nyqvist D, Giampietro C, Dejana E (2008) Deciphering the functional role of endothelial junctions by using in vivo models. EMBO Rep 9 (8):742-747. doi:embor2008123 [pii]
10.1038/embor.2008.123
38. Hewat EA, Durmort C, Jacquamet L, Concord E, Gulino-Debrac D (2007) Architecture of the VE-cadherin hexamer. J Mol Biol 365 (3):744-751. doi:S0022-2836(06)01432-X [pii]
10.1016/j.jmb.2006.10.052
39. Chitaev NA, Troyanovsky SM (1998) Adhesive but not lateral E-cadherin complexes require calcium and catenins for their formation. J Cell Biol 142 (3):837-846
40. Dejana E, Orsenigo F, Molendini C, Baluk P, McDonald DM (2009) Organization and signaling of endothelial cell-to-cell junctions in various regions of the blood and lymphatic vascular trees. Cell Tissue Res 335 (1):17-25. doi:10.1007/s00441-008-0694-5

41. Nelson CM, Jean RP, Tan JL, Liu WF, Sniadecki NJ, Spector AA, Chen CS (2005) Emergent patterns of growth controlled by multicellular form and mechanics. Proc Natl Acad Sci U S A 102 (33):11594-11599. doi:0502575102 [pii]
10.1073/pnas.0502575102
42. Wallez Y, Huber P (2008) Endothelial adherens and tight junctions in vascular homeostasis, inflammation and angiogenesis. Biochim Biophys Acta 1778 (3):794-809. doi:S0005-2736(07)00346-X [pii]
10.1016/j.bbamem.2007.09.003
43. Nelson PJ, Daniel TO (2002) Emerging targets: molecular mechanisms of cell contact-mediated growth control. Kidney Int 61 (1 Suppl):S99-105. doi:kid017 [pii]
10.1046/j.1523-1755.2002.0610s1099.x
44. Tille JC, Wood J, Mandriota SJ, Schnell C, Ferrari S, Mestan J, Zhu Z, Witte L, Pepper MS (2001) Vascular endothelial growth factor (VEGF) receptor-2 antagonists inhibit VEGF- and basic fibroblast growth factor-induced angiogenesis in vivo and in vitro. J Pharmacol Exp Ther 299 (3):1073-1085
45. Seghezzi G, Patel S, Ren CJ, Gualandris A, Pintucci G, Robbins ES, Shapiro RL, Galloway AC, Rifkin DB, Mignatti P (1998) Fibroblast growth factor-2 (FGF-2) induces vascular endothelial growth factor (VEGF) expression in the endothelial cells of forming capillaries: an autocrine mechanism contributing to angiogenesis. J Cell Biol 141 (7):1659-1673
46. Elson DA, Thurston G, Huang LE, Ginzinger DG, McDonald DM, Johnson RS, Arbeit JM (2001) Induction of hypervascularity without leakage or inflammation in transgenic mice overexpressing hypoxia-inducible factor-1alpha. Genes Dev 15 (19):2520-2532. doi:10.1101/gad.914801
47. Richard DE, Berra E, Pouyssegur J (2000) Nonhypoxic pathway mediates the induction of hypoxia-inducible factor 1alpha in vascular smooth muscle cells. J Biol Chem 275 (35):26765-26771. doi:10.1074/jbc.M003325200
M003325200 [pii]
48. Fukuda R, Hirota K, Fan F, Jung YD, Ellis LM, Semenza GL (2002) Insulin-like growth factor 1 induces hypoxia-inducible factor 1-mediated vascular endothelial growth factor expression, which is dependent on MAP kinase and phosphatidylinositol 3-kinase signaling in colon cancer cells. J Biol Chem 277 (41):38205-38211. doi:10.1074/jbc.M203781200
M203781200 [pii]
49. Lee S, Chen TT, Barber CL, Jordan MC, Murdock J, Desai S, Ferrara N, Nagy A, Roos KP, Iruela-Arispe ML (2007) Autocrine VEGF signaling is required for vascular homeostasis. Cell 130 (4):691-703. doi:S0092-8674(07)00905-1 [pii]
10.1016/j.cell.2007.06.054
50. Fong GH (2009) Regulation of angiogenesis by oxygen sensing mechanisms. J Mol Med (Berl) 87 (6):549-560. doi:10.1007/s00109-009-0458-z
51. Ozawa CR, Banfi A, Glazer NL, Thurston G, Springer ML, Kraft PE, McDonald DM, Blau HM (2004) Microenvironmental VEGF concentration, not total dose, determines a threshold between normal and aberrant angiogenesis. J Clin Invest 113 (4):516-527. doi:10.1172/JCI18420
52. Shim K, Minowada G, Coling DE, Martin GR (2005) Sprouty2, a mouse deafness gene, regulates cell fate decisions in the auditory sensory epithelium by antagonizing FGF signaling. Dev Cell 8 (4):553-564. doi:S1534-5807(05)00079-1 [pii]

10.1016/j.devcel.2005.02.009
53. Klein OD, Minowada G, Peterkova R, Kangas A, Yu BD, Lesot H, Peterka M, Jernvall J, Martin GR (2006) Sprouty genes control diastema tooth development via bidirectional antagonism of epithelial-mesenchymal FGF signaling. Dev Cell 11 (2):181-190. doi:S1534-5807(06)00255-3 [pii]
10.1016/j.devcel.2006.05.014
54. Peterkova R, Churava S, Lesot H, Rothova M, Prochazka J, Peterka M, Klein OD (2009) Revitalization of a diastemal tooth primordium in Spry2 null mice results from increased proliferation and decreased apoptosis. J Exp Zool B Mol Dev Evol 312B (4):292-308. doi:10.1002/jez.b.21266
55. Matsumura K, Taketomi T, Yoshizaki K, Arai S, Sanui T, Yoshiga D, Yoshimura A, Nakamura S (2011) Sprouty2 controls proliferation of palate mesenchymal cells via fibroblast growth factor signaling. Biochem Biophys Res Commun 404 (4):1076-1082. doi:S0006-291X(10)02354-5 [pii]
10.1016/j.bbrc.2010.12.116
56. Folkman J, Merler E, Abernathy C, Williams G (1971) Isolation of a tumor factor responsible for angiogenesis. J Exp Med 133 (2):275-288
57. Murakami M, Nguyen LT, Zhuang ZW, Moodie KL, Carmeliet P, Stan RV, Simons M (2008) The FGF system has a key role in regulating vascular integrity. J Clin Invest 118 (10):3355-3366. doi:10.1172/JCI35298
58. Hackett PH, Roach RC (2004) High altitude cerebral edema. High Alt Med Biol 5 (2):136-146. doi:10.1089/1527029041352054
59. Carmeliet P, Jain RK (2000) Angiogenesis in cancer and other diseases. Nature 407 (6801):249-257. doi:10.1038/35025220

Figure legends

Fig. 1 Generation of Spry2 knockout MAECs (A) MAECs (♀) were isolated from floxed Spry2 female mice. The cells were then exposed to Ade-Cre-GFP Adenovirus or the corresponding Adenovirus without Cre. (B) GFP expression 24 hours after transfection with either Ade-Cre-GFP ($Spry2^{-/-}$) or the corresponding control virus Ade-CMV-GFP ($Spry2^{fl/fl}$) (scale bar 100 μm). (C,D) Efficient knockout of Spry2 was confirmed by qRT-PCR analysis (error bars show mean +/- s.e.m.; ***P<0.001; n=3) (B) and immunoblotting analysis (C). β-actin was used as loading control

Fig. 2 Spry2 knockout results in a loss of contact inhibition and endothelial monolayer integrity (A1,A2) Micrographs (scale bar 100 μm) display $Spry2^{fl/fl}$ (A1) and $Spry2^{-/-}$ (A2) MAECs (♀) plated at confluence and grown for 48 hours in the presence of 1% FCS both with and without FGF2 (25 ng/ml). Magnifications (scale bar 50 μm) of FGF2-treated $Spry2^{fl/fl}$ and $Spry2^{-/-}$ cells are shown at the bottom of the panel. (B) Modulation in monolayer permeability of $Spry2^{fl/fl}$ and $Spry2^{-/-}$ cells in the presence of FGF2. Cells were seeded at confluence on a well insert in the presence of 1% FCS with and without FGF2 (25 ng/ml). The permeability of the monolayer to 70 kDa FITC-dextran after 10 min was evaluated by measuring fluorescence of the lower well. Bars show values as fold change of control +/- s.e.m.; ***P<0.001; n=4. (C) $Spry2^{-/-}$ cells lack contact inhibition. Cells were plated at the indicated cell densities and grown for 48 hours in the presence of 1% FCS both with and without FGF2 (25 ng/ml). Bars show the FGF2-induced proliferation of $Spry2^{fl/fl}$ and $Spry2^{-/-}$ MAECs (♀) normalized to the unstimulated cell at the indicated plating densities +/- s.e.m.; ***P<0.001 vs. 3,000 cells/cm^2 + FGF2; ##P<0.01; ###P<0.001 $Spry2^{fl/fl}$ vs. $Spry2^{-/-}$; ns=non-significant; n=3

Fig. 3 High cell density induces Spry2 (A) Representative micrographs of MAECs (♂) plated at different cell numbers (scale bar 100 μm). (B) MAECs (♂) were subjected to immunoblotting after 24 hours of serum starvation. (C) mRNA expression of sparse (3,000 cells/cm^2) and confluent cells (50,000 cells/cm^2) was analyzed by qRT-PCR and compared to the corresponding protein expression (Spry2/β-Actin) of sparse and confluent cells (MAECs ♂). The present graphs summarize at least three independent experiments. The values shown are means +/- s.e.m.; **P<0.01; ***P<0.001 vs. 3,000 cells/cm^2. (D,E) Cells (MAECs ♂) growing to confluence increase Spry2. (D) Micrographs (scale bar 100 μm) of MAECs plated at sparse condition (3,000 cells/cm^2) and grown for the indicated time. (E) Cell (MAECs ♂) samples were collected at the indicated times and Spry2 and β-actin levels were analyzed by immunoblotting

Fig. 4 Hypoxia increases Spry2 protein expression (A) Cells (MAECs ♂) growing to confluence become hypoxic. Cell samples were collected at the indicated times and analyzed for Hif-1α and β-actin protein expression. (B) Real-time measurement of the oxygen consumption of MAECs (♂) growing to confluence (initially plated at sparse density; 3,000 cells/cm^2) (C) Cells (MAECs ♂) were grown in 10% FCS for 24 hours and then either collected or starved for 24 hours, and then Spry2 levels were determined by immunoblotting. Three independent experiments, normalized to β-actin expression, are summarized in a graph that shows densitometric quantification of the immunoblotting signals (**P<0.01). (D) In parallel experiments, real time oxygen consumption of growing and quiescent cells (MAECs (♂) plated at confluence; 50,000 cells/cm^2). After 24 hours, either serum free or media with 10 % FCS was added for additional 24 hours to the cells (indicated

with a dashed line). (D) MAECs (♂) were grown for 24 hours and then starved and grown under either hypoxic (1% O_2) or normoxic (21 % O_2) conditions before lysis and immunoblotting for Spry2, Hif-1α and β-actin. Three independent experiments, normalized to β-actin expression, are summarized in a graph that shows densitometric quantification of the bands (**P<0.01). (H) mRNA was collected from MAECs (♂) grown for 24 hours and then starved and grown under either hypoxic (1% O_2) or normoxic (21 % O_2) conditions and analyzed for Spry2 expression by qRT-PCR. Values were normalized to GAPDH; n=4

Fig. 5 Disruption of cell-cell contacts decrease Spry2 protein levels (A, panels 1-3) Micrographs (scale bar 100 μm) of MAECs (♂) plated at confluence and treated with PBS (the control) or EGTA for the indicated time. (A, panel 4) After 3 hours, EGTA was replaced by fresh growth media, and cells were grown for an additional 24 hours. (B) Spry2 expression after EGTA treatment. MAECs (♂) were collected after the indicated incubation time with PBS (control) or EGTA or 24 hours after replacement of EGTA with fresh media (3.0 + 24). (C) Cells were plated at confluence, and total resistance was measured in real time by ECIS. When cells reached a steady plateau in resistance (baseline), either EGTA or PBS (control) was added to the cells. After 8 hours, new media was added to all cells and the time point was set to zero. (D) MAECs (♂) were treated with either EGTA or BAPTA-AM for 3 hours, and Spry2 and β-actin expression were analyzed by immunoblotting. (E) In parallel experiments, total RNA was isolated from MAECs (♂) that had been treated with EGTA, BAPTA-AM, or PBS. Spry2 mRNA levels were determined by using qRT-PCR and normalized to GAPDH. The values shown are means +/- s.e.m.; n=3. (F) MAECs (♂) were plated at confluence and then treated with either TNFα (50 ng/ml), thrombin (10 u/ml) or PBS for 3 hours. Cells were then lysed and analyzed for Spry2 and β-actin expression by immunoblotting. (G) In parallel experiments, total resistance was measured in real time by ECIS. When the cells reached the plateau, either TNFα (50 ng/ml), thrombin (10 u/ml) or PBS was added for the indicated time

Fig. 6 Inhibition of Erk1/2 signaling restores wild type morphology of the $Spry2^{-/-}$monolayer (A) High cell density-induced Spry2 correlates with decreased Erk1/2 phosphorylation. Sparse (3,000 cells/cm^2) or confluent MAECs (♂) (50,000 cells/cm^2) were starved and then treated with FGF2 (25 ng/ml) or PBS for 24 hours before lysis and immunoblotting. Relative phosphorylation levels of Erk1/2 were quantified by densitometry. Bars show values as fold change of unstimulated sparse cells +/-s.e.m.; **P<0.01; ***P<0.001; n=3. (B) Micrographs displaying $Spry2^{fl/fl}$ and $Spry2^{-/-}$ MAECs (♀) plated at confluence in the absence or presence of FGF2 (25 ng/ml) and then grown for 48 hours. Where indicated, cells were incubated with U0126 (5 μM) 1 hour prior the addition of FGF2 (scale bar 100 μm). (C1) MAECs (♀) were plated at confluence in the presence or absence of FGF2 both with and without pre-incubation with U0126 (5 μM). Cells were collected 4 hours after seeding and phosphorylated Erk1/2 (p-Erk1/2), total Erk1/2 (t-Erk1/2), Spry2 and β-actin were analyzed by immunoblotting. (C2) Relative phosphorylation levels of Erk1/2 were quantified by densitometry. Bars show values as fold change of FGF2-stimulated $Spry2^{fl/fl}$ cells +/- s.e.m.; **P<0.01; n=3

Fig. 7 A working model for the regulation of Spry2-dependent endothelial quiescence and integrity (A) In wild type endothelial cells ($Spry2^{fl/fl}$), Spry2 is upregulated by increasing cell density via transient hypoxia in subconfluent cells and cell-cell contacts in confluent cells via a yet unknown mechanism. Spry2 expression allows the endothelial monolayer to retain its integrity and cell quiescence, upon FGF stimulation. (B) In the

absence of Spry2 (Spry2$^{-/-}$), FGF signaling extensively activates Erk1/2. Erk1/2 elicits an endothelial phenotype change from cobble-stone to spindle-shape endothelial cells, induces proliferation, and increases permeability

Supplementary figure 1 Male and female MAECs show similar FGF2-Erk1/2 signaling and density dependent Spry2 expression (A) Confluent female (♀) and male (♂) MAECs were starved and stimulated with FGF2 for the indicated time. The cells were then lysed and analyzed for ERK1/2 phosphorylation and total Erk1/2 expression. Relative phosphorylation levels of Erk1/2 were quantified by densitometry. Bars show values as fold change of unstimulated cells +/- s.e.m. n=3. (B) Basal Spry2 expression and Erk1/2 activity in sparse and confluent female and male MAECs. Cells were plated at sparse (3,000 cells/cm^2) or confluent conditions (50,000 cells/cm^2), starved, lysed and analyzed by immunoblotting

Summary of all changes in the figures of the revised manuscript:

Figure 5

Panel F now displays Spry2 protein expression 3 hours after addition of either TNFα, thrombin or PBS (control) to confluent cells.

Panel G now displays the normalized resistance of confluent cells treated with either TNFα, thrombin or PBS (control) for the indicated time.

Figure_1
Click here to download high resolution image

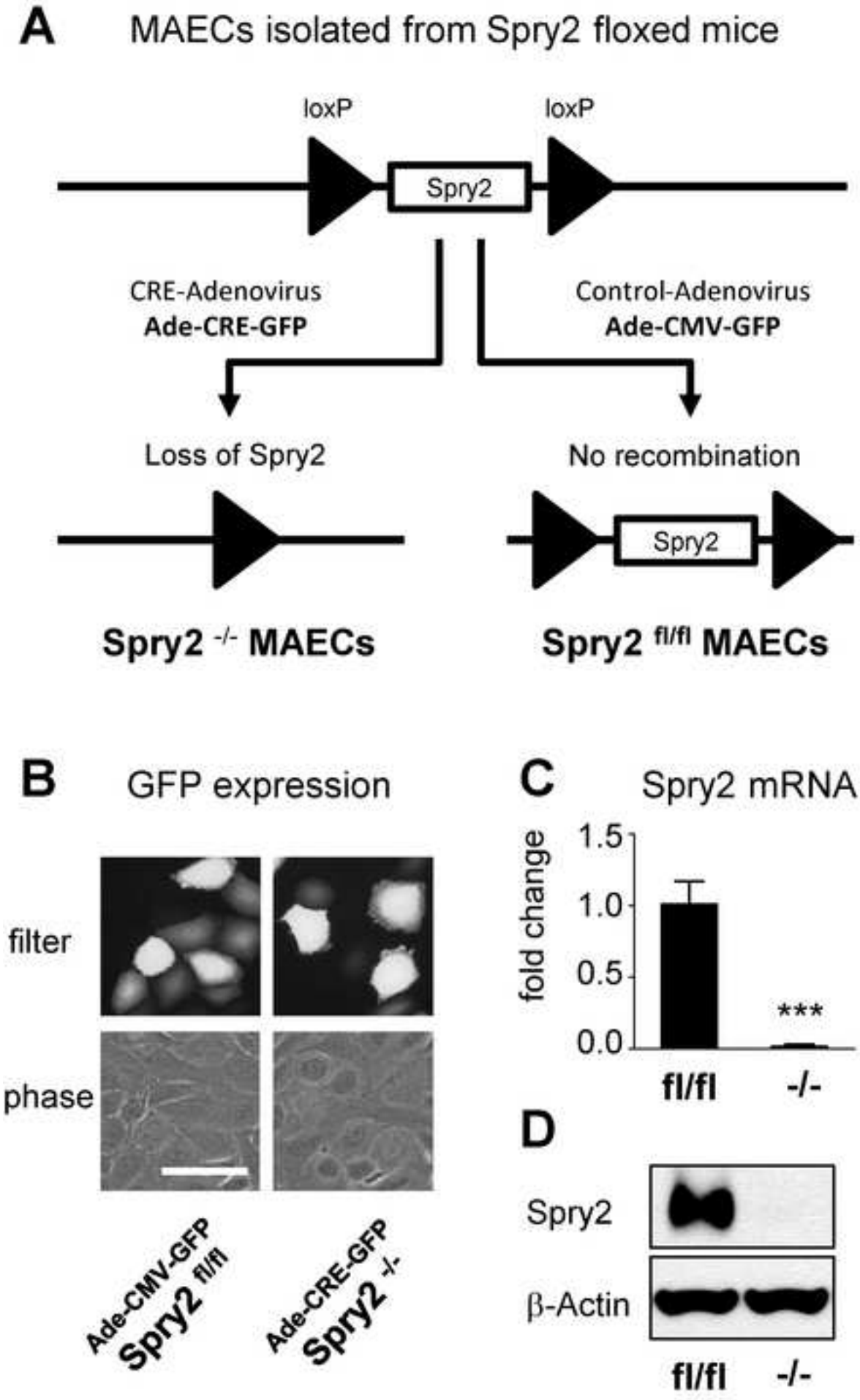

Figure_2
Click here to download high resolution image

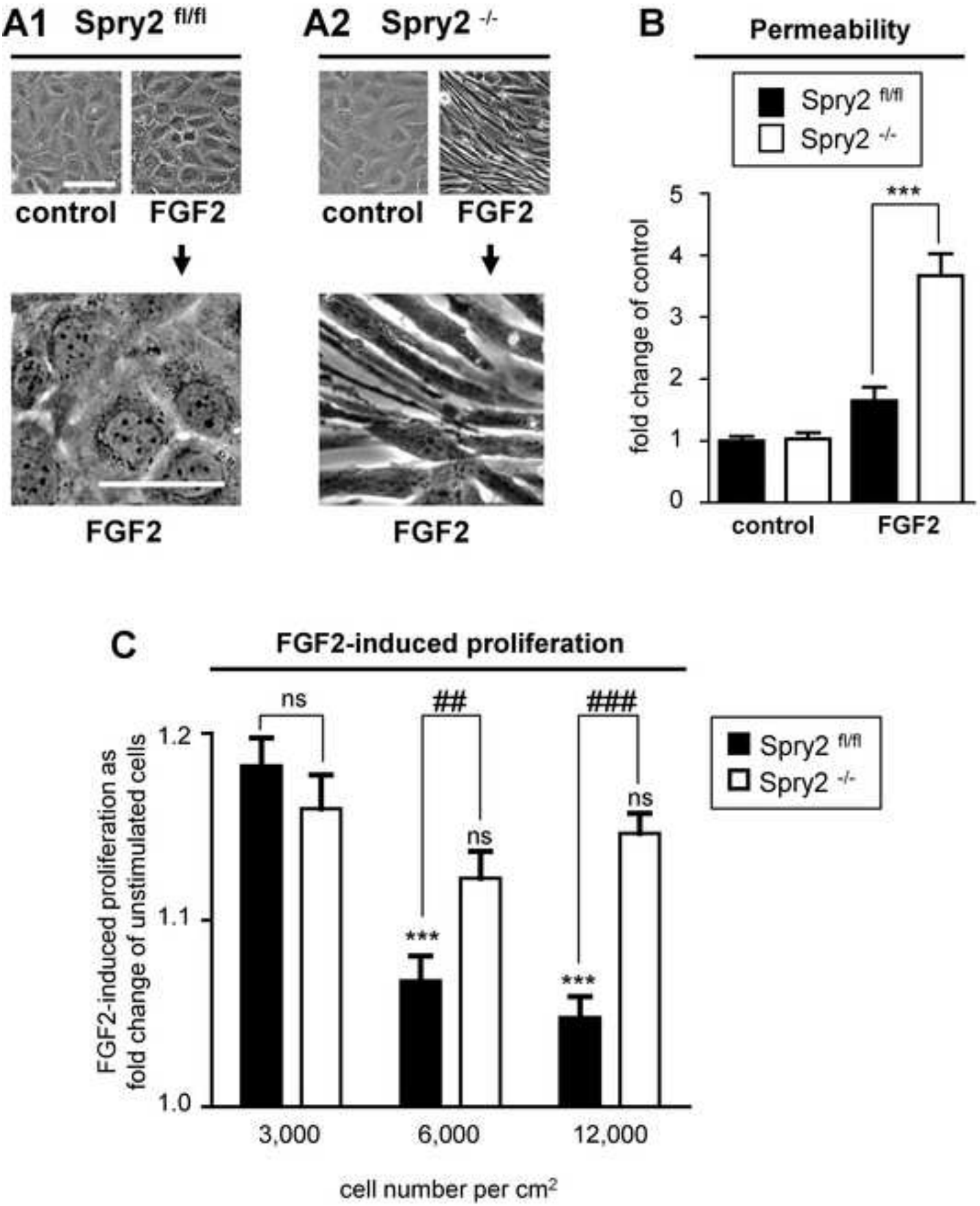

Figure_3
Click here to download high resolution image

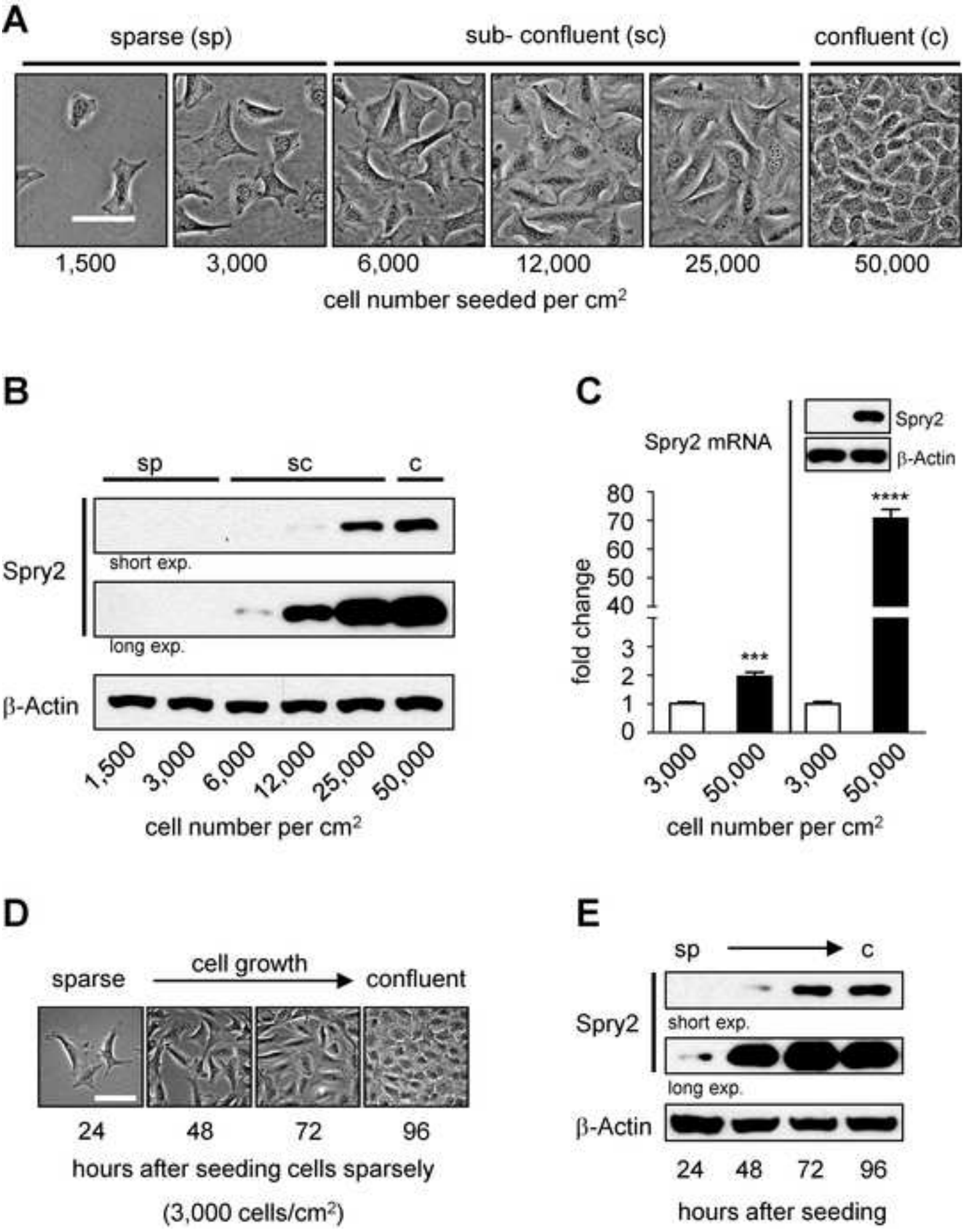

Figure_4
Click here to download high resolution image

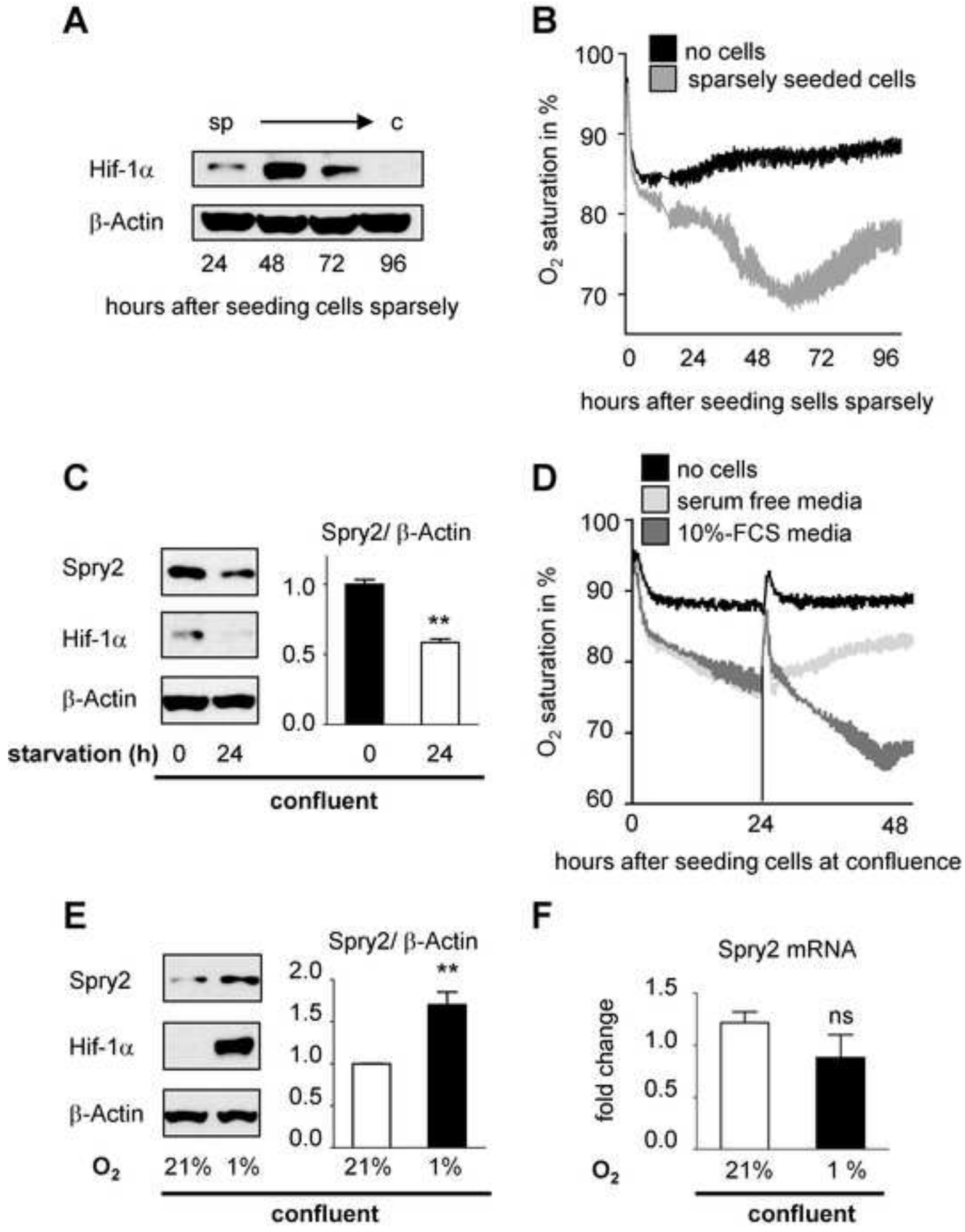

Figure_5
Click here to download high resolution image

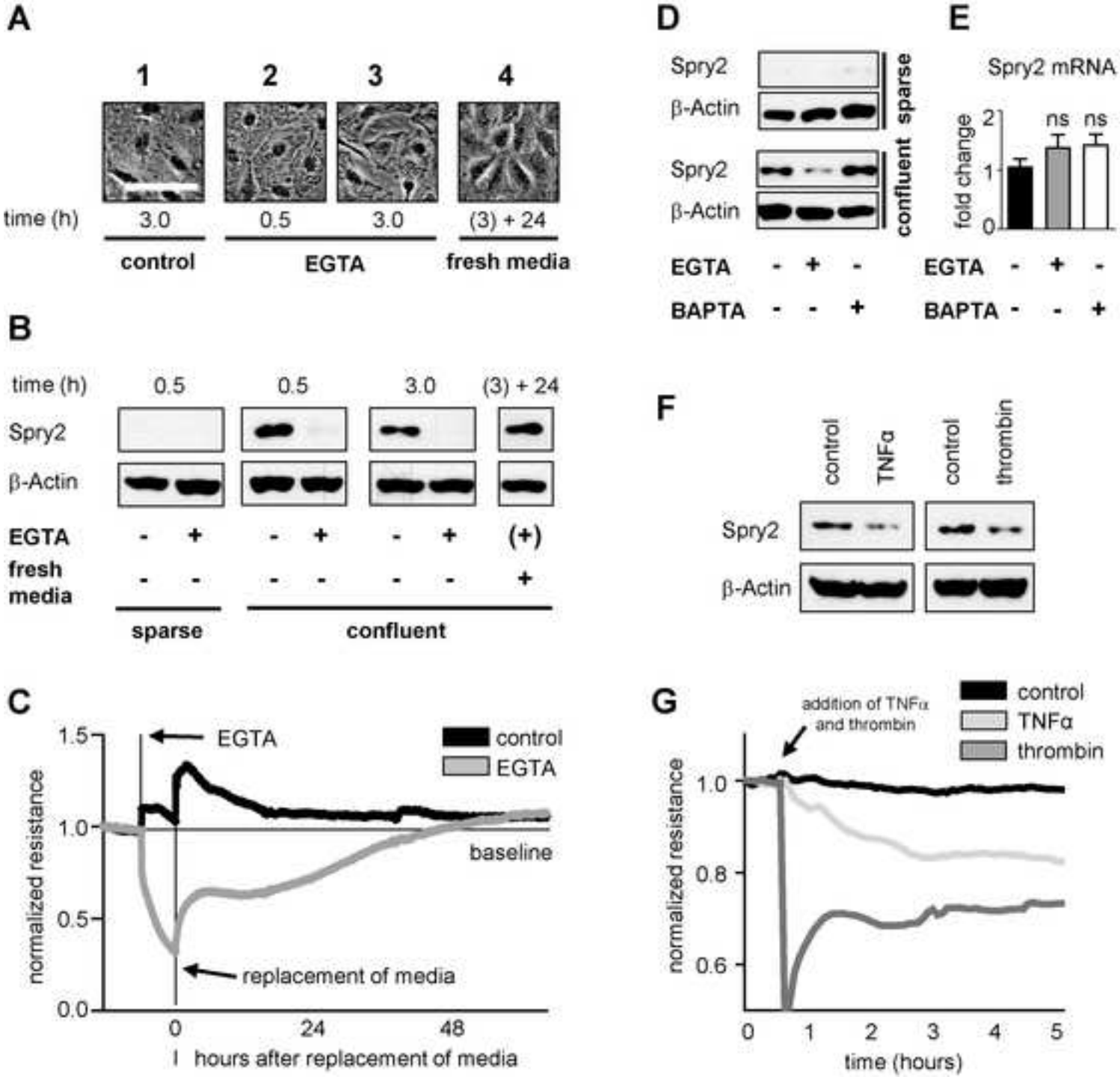

Figure_6
Click here to download high resolution image

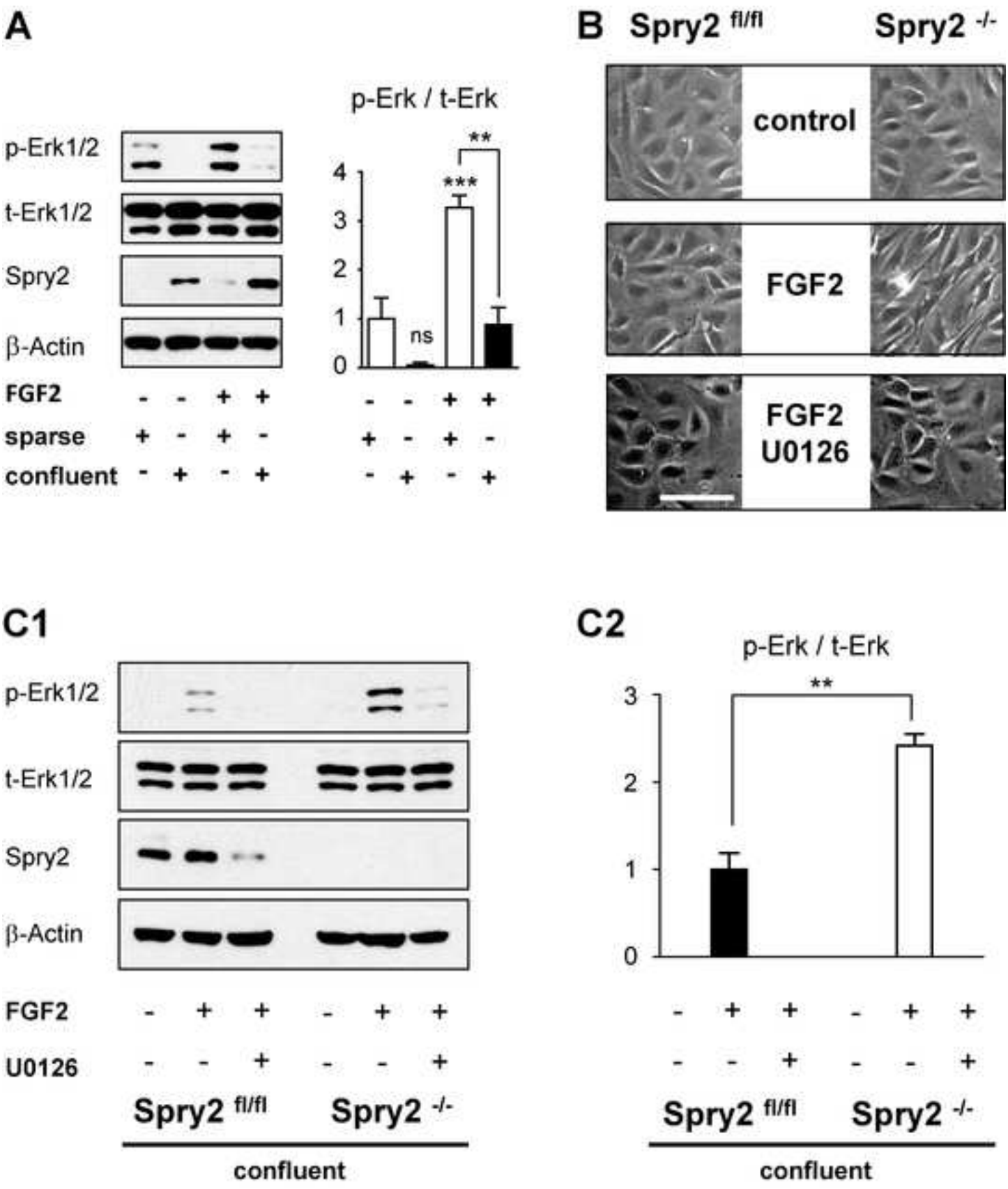

Figure_7
Click here to download high resolution image

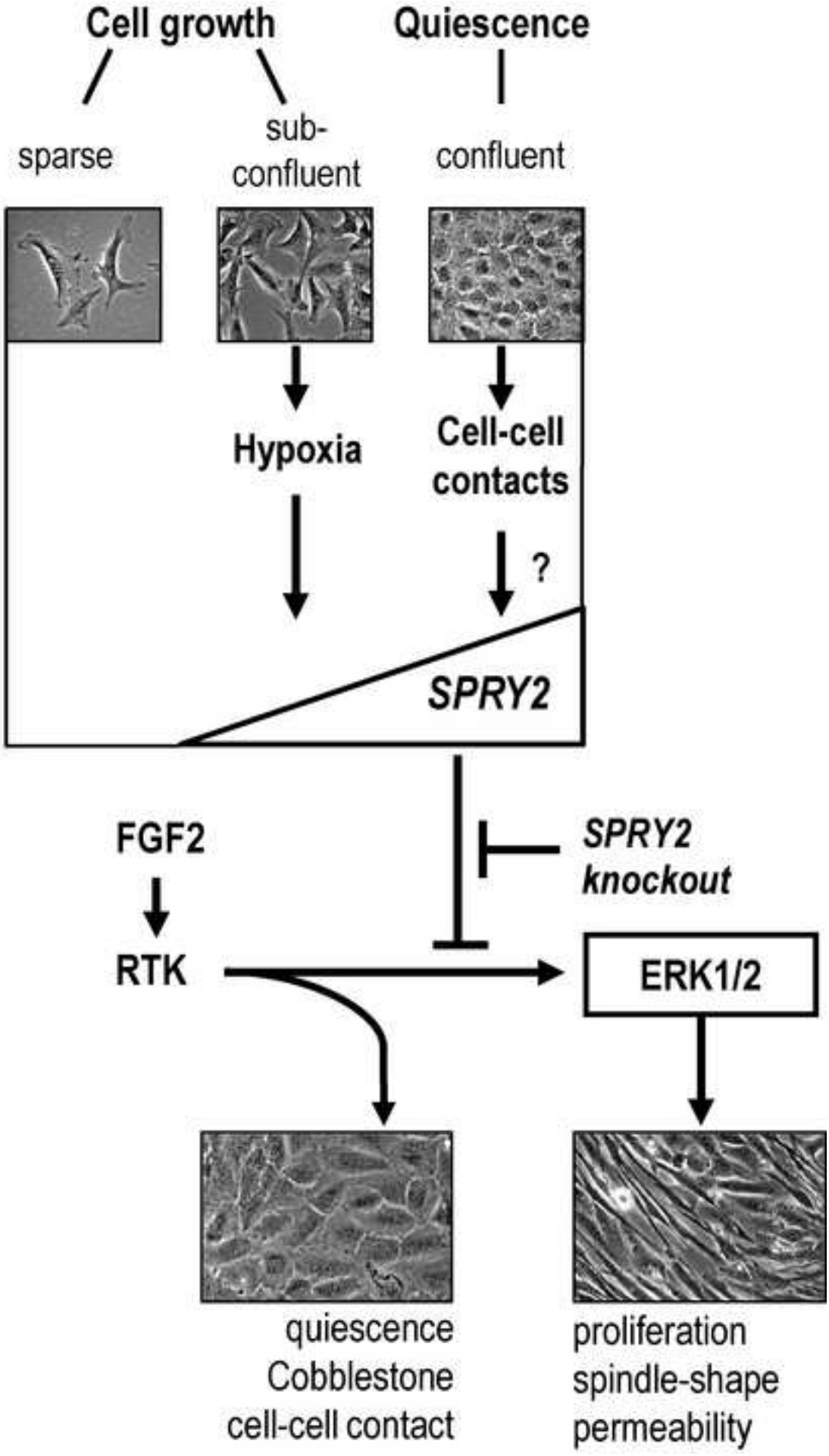

Supplementary_Figure_1

Click here to download Electronic supplementary material: Suppl_Fig_1.tif